

Biometric Identification via Eye Movement Scanpaths in Reading

Corey Holland (ch1570@txstate.edu), Oleg V. Komogortsev (ok11@txstate.edu)

Abstract

This paper presents an objective evaluation of various eye movement-based biometric features and their ability to accurately and precisely distinguish unique individuals. Eye movements are uniquely counterfeit resistant due to the complex neurological interactions and extraocular muscle properties involved in their generation. Considered biometric candidates cover a number of basic eye movements and their aggregated scanpath characteristics, including: fixation count, average fixation duration, average saccade amplitudes, average saccade velocities, average saccade peak velocities, the velocity waveform, scanpath length, scanpath area, regions of interest, scanpath inflections, the amplitude-duration relationship, the main sequence relationship, and the pairwise distance between fixations. As well, an information fusion method for combining these metrics into a single identification algorithm is presented. With limited testing this method was able to identify subjects with an equal error rate (EER) of 27%. These results indicate that scanpath-based biometric identification holds promise as a behavioral biometric technique.

1. Introduction

Biometric identification refers to the automated process of extracting, processing, and comparing certain distinctive physical or behavioral characteristics, for the purposes of uniquely identifying a given individual [7]. Biometrics has and continues to maintain a crucial role in the fields of law enforcement, criminal justice, and corporate and personal security. Suspect identification, criminal conviction, access restriction, and personalized interfaces constitute only a small subset of the many and varied applications of biometrics in modern society.

As technology advances, however, biometric traits are becoming easier to reproduce, circumventing the purposes of biometric identification techniques and leaving gaps in the efficacy of the systems that use them [18]. To combat this, improvements must continue to be made to existing biometric systems to increase the accuracy and specificity

of biometric identification techniques.

There are a wide range of physical and behavioral traits that can be used to identify an individual, often involving the hands [3], face [13], eyes [4], or ears [1]. The eyes in particular offer a variety of physical (iris) and behavioral (eye movements) properties that make them ideal for the purposes of biometric identification, due to their high specificity and the complex mechanical logistics of reproduction [11].

Eye movements are highly counterfeit resistant, as they depend largely on the brain activity and extraocular muscle properties of an individual. As a result, with our current knowledge of the human brain and extraocular muscle structure, it is not possible to accurately replicate eye movements outside of a living human.

While there has been some research into the general applicability of eye movements as a behavioral biometric [8, 23], the error rates produced by current methods of eye movement analysis tend to be much higher than those of accepted biometric systems. For this reason, more research is required to identify eye movement features, and methods of extraction, that are able to provide a higher level of specificity and noise tolerance. In this paper we consider various methods of eye movement pattern (scanpath) analysis and their ability to accurately distinguish between unique individuals in the context of biometric identification.

2. Background

The term scanpath refers to the spatial path formed by a sequence of fixations and saccades. Fixations occur when the eye is held in a relatively stable position, allowing heightened visual acuity on an object of interest. Saccades occur when the eye rotates quickly (with velocities reaching as high as 700°/s) between points of fixation, with almost no visual acuity maintained during rotation [12].

Scanpath theory is the idea that individuals tend to repeat certain scanpath trajectories during repeated viewings of a given pattern. This phenomenon was first investigated by Noton and Stark [14], where it was found that the general scanpath displayed by a subject during the first viewing of a pattern was repeated in the initial eye movements of roughly 65% of subsequent viewings.

As well, it has been noted by various sources [14, 16, 22] that the scanpaths produced for a given stimulus pattern tend to vary for different subjects. The hypothesized explanation being that these scanpaths are formed in memory during the initial viewing of a pattern.

These inherent properties of scanpaths – subconscious reproduction, variation by subject, variation by stimulus – make them promising candidates as a behavioral biometric. In this paper, we investigate specifically the scanpaths formed during reading.

The reading process presents an instance of high usability, as it is a fairly common activity which should be familiar to most subjects. For an unfamiliar text, reading is also an active cognitive process whose pace and direction are set by the individual subject's knowledge and experience with similar texts [15, 16]. This cognitive nature of reading forces the subject to concentrate on the material rather than the task, producing more realistic and natural eye movements.

3. Biometrics via Scanpath Analysis

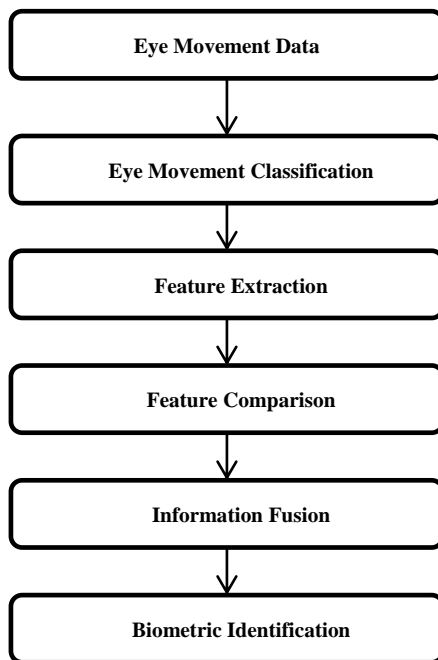


Figure 1: Biometrics via scanpath analysis.

Figure 1 provides an overview of our approach to biometrics via scanpath analysis. The raw Eye Movement Data produced during various recordings is supplied to the Eye Movement Classification module which identifies, filters, and merges the data points that describe the unique fixations/saccades present in each. Merged fixation and saccade groups are then sent to the Feature Extraction module for analysis, where scanpath features are calculated. In comparing two scanpaths, the scanpath

features and fixation groups of each recording are sent to the Feature Comparison module, in which similarity scores are calculated for the various scanpath features, and a pairwise distance comparison is performed on opposing fixation points. The various similarity scores are then supplied to the Information Fusion module to combine them into a single similarity score that can be used for Biometric Identification.

3.1. Eye Movement Classification

The raw eye movement signal, shown in Figure 2, produced by an eye tracker presents a great deal of information, much more in fact than is practically necessary during scanpath analysis. It would not be practical, for instance, to compare 100,000+ unique data points when the number of fixations/saccades represented by that data does not exceed 500. As well, this data often contains extraneous noise caused by blinks and the inherent inaccuracy of the eye tracking system. As a result, this signal must be processed and filtered to provide accurate and useful information.

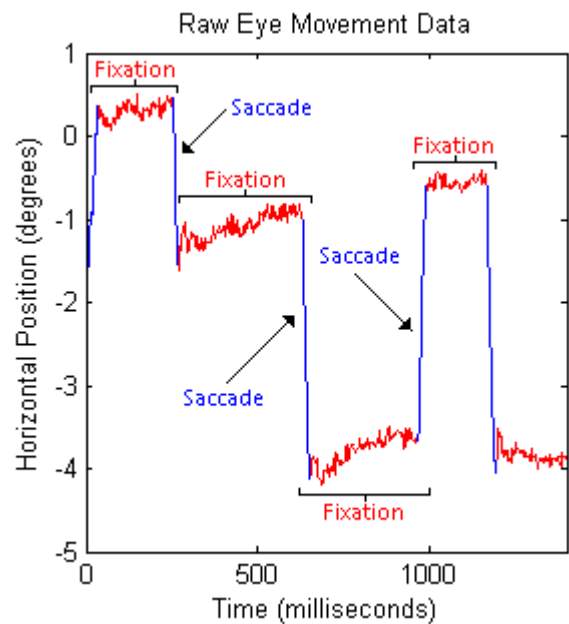
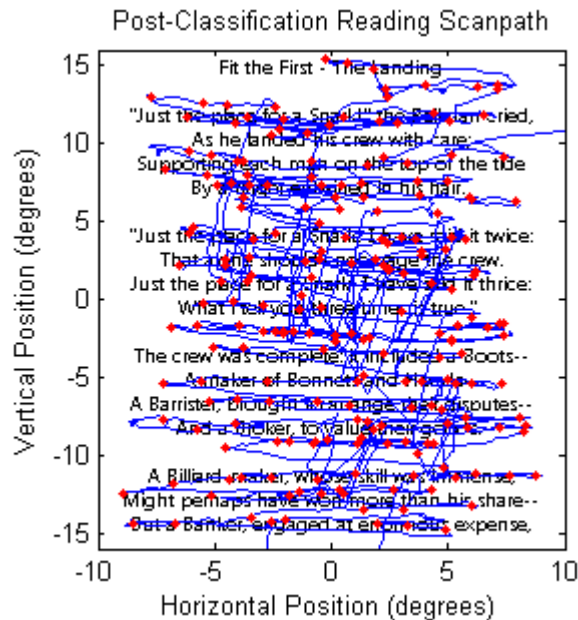


Figure 2: Raw eye movement signal.

To reduce the data set to the basic fixations and saccades that form the scanpath, a velocity threshold algorithm [10] was employed to classify individual points with a velocity greater than $50^\circ/\text{sec}$ as saccades, where all remaining points were assumed to be fixations. Following the classification process, a micro-saccade filter re-classified saccades with amplitude less than 0.5° as fixations, and a micro-fixation filter re-classified fixations with a duration less than 100 milliseconds as saccades.

300 Fixation and saccade groups, shown in Figure 3, were
 301 then merged. Fixation data included: start time, duration,
 302 and positional centroid. Saccade data included: start time,
 303 duration, amplitude, velocity, and peak velocity.



327 **Figure 3: Example reading scanpath.**

328 As a side-note, in all recordings produced in the current
 329 experiment the number of fixations and saccades was less
 330 than the square root of the total number of data points; this
 331 information was useful for improving the performance of
 332 processing algorithms. For example, an eye movement
 333 recording containing 60,000 data points often contained
 334 less than 245 fixations and 245 saccades. Note also that this
 335 relation is heavily dependent on the frequency of data
 336 collection.

337 3.2. Feature Extraction

338 The processed fixation and saccade groups essentially
 339 describe the scanpath of a recording. By considering the
 340 properties of the scanpath, we hope to identify scanpath
 341 features that hold promise as biometric indicators. To this
 342 end, a number of eye movement metrics were calculated for
 343 each recording based on the properties of its unique
 344 scanpath.

345 Basic eye movement metrics considered include:
 346 fixation count, average fixation duration, average vectorial
 347 saccade amplitude, average horizontal saccade amplitude,
 348 average vertical saccade amplitude, average vectorial
 349 saccade velocity, average vectorial saccade peak velocity,
 and the velocity waveform indicator (Q).

More complex metrics, resulting from the aggregated
 scanpath data, include: scanpath length, scanpath area,

350 regions of interest, inflection count, and slope coefficients
 351 of the amplitude-duration and main sequence relationships.

352 **Fixation Count.** Fixation count is indicative of the number
 353 of objects processed by the subject [5], and was measured
 354 simply as the total number of fixations contained within the
 355 scanpath.
 356

357 **Average Fixation Duration.** Average fixation duration is
 358 indicative of the amount of time a subject spends
 359 interpreting an object [5], and was measured as the sum of
 360 fixation durations over the fixation count.
 361

362 **Average Vectorial Saccade Amplitude.** There is a noted
 363 tendency for saccades to maintain similar amplitudes
 364 during reading [22], average saccade amplitude was
 365 considered as a candidate biometric feature under the
 366 assumption that differences in amplitude may be apparent
 367 between subjects. Average vectorial saccade amplitude was
 368 measured as the sum of vectorial saccade amplitudes over
 369 the total number of saccades, where the vectorial amplitude
 370 of a saccade was defined as the Euclidean norm of the
 371 horizontal and vertical amplitudes, according to the
 372 equation:

$$373 \text{Vectorial Average} = \frac{\sum_{i=1}^n \sqrt{x_i^2 + y_i^2}}{n} \quad (1) \quad 374$$

375 **Average Horizontal Saccade Amplitude.** Horizontal
 376 saccade amplitude was considered separately as these are
 377 more indicative of between-word saccades. Average
 378 horizontal saccade amplitude was measured as the sum of
 379 horizontal saccade amplitudes greater than 0.5° over the
 380 total number of horizontal saccades with amplitude greater
 381 than 0.5° .
 382

383 **Average Vertical Saccade Amplitude.** Vertical saccade
 384 amplitude was considered separately as these are more
 385 indicative of between-line saccades. Average vertical
 386 saccade amplitude was measured as the sum of vertical
 387 saccade amplitudes greater than 0.5° over the total number
 388 of vertical saccades with amplitude greater than 0.5° .
 389

390 **Average Vectorial Saccade Velocity.** Average vectorial
 391 saccade velocity as measured as the sum of vectorial
 392 saccade velocities over the total number of saccades, where
 393 the vectorial velocity of a saccade was defined as the
 394 Euclidean norm of the horizontal and vertical velocities.
 395

396 **Average Vectorial Saccade Peak Velocity.** Average
 397 vectorial saccade peak velocity was measured as the sum of
 398 vectorial saccade peak velocities over the total number of
 399 saccades, where the vectorial peak velocity of a saccade
 was defined as the Euclidean norm of the horizontal and
 vertical peak velocities.

Velocity Waveform Indicator (Q). We use the term velocity waveform indicator (Q) to refer to the ratio of peak velocity to average velocity of a given saccade [12]. In normal human saccades this value is roughly constant at 1.6, though it is assumed that this is subject to some amount of variation similar to the amplitude-duration and main sequence relationships. A rough estimate of this value was obtained from the ratio of the average vectorial peak velocity over the average vectorial velocity.

Scanpath Length. Scanpath length is indicative of the efficiency of visual search [5], and was considered as a candidate biometric feature under the assumption that visual search is dependent on the subject's familiarity with similar patterns/content. Scanpath length was measured as the sum of absolute distances between the vectorial centroid of fixation points, where the vectorial centroid was defined as the Euclidean norm of the horizontal and vertical centroid positions, according to the equation:

$$\text{Scanpath Length} = \sum_{i=2}^n \left| \sqrt{x_i^2 + y_i^2} - \sqrt{x_{i-1}^2 + y_{i-1}^2} \right| \quad (2)$$

Scanpath Area. Scanpath area was measured as the area of the convex hull formed by fixation points, as described by Goldberg and Kotval [5]. Scanpath area is similar to scanpath length in its indication of visual search efficiency, but is less sensitive to localized searching. That is, a scanpath may have a large length while only covering a small area.

Regions of Interest. Regions of interest was measured as the total number of spatially unique regions identified after applying a spatial mean shift clustering algorithm [20] to the fixation points of the scanpath, using a sigma value of 2° and convergence resolution of 0.1° .

Inflection Count. Inflections occur when the scanpath changes direction, in reading there are a certain amount of "forced" inflections that are necessary to progress through the text, but general differences in inflection count are indicative of attentional shifts. Inflection count was measured as the number of saccades in which the horizontal and/or vertical velocity changes signs, according to the following algorithm:

1. Inflections = 0
2. $i = 2$
3. While $i < \text{Saccade Count}$:
4. If $\text{sign}(\text{Velocity}_i) \neq \text{sign}(\text{Velocity}_{i-1})$:
5. Inflections = Inflections + 1
6. End if
7. $i = i + 1$
8. End while

Coefficient of the Amplitude-Duration Relationship. The amplitude-duration relationship varies from person to person, and describes the tendency for saccade duration to increase linearly with amplitude [12], according to the equation:

$$\text{Duration} = C \times |\text{Amplitude}| + \text{Duration}_{\min} \quad (3)$$

To calculate the slope coefficient of this relationship, a data set was constructed from the saccade groups such that x-column data contained the larger absolute component (horizontal or vertical) amplitude and y-column data contained the respective saccade duration.

The slope coefficient of the amplitude-duration relationship was obtained from a linear regression of this data set.

Coefficient of the Main Sequence Relationship. The main sequence relationship varies from person to person, and describes the tendency for saccade peak velocity to increase exponentially with amplitude [2], according to the equation:

$$\text{Peak Velocity} = \text{Velocity}_{\max} \left(1 - e^{-\frac{|\text{Amplitude}|}{c}} \right) \quad (4)$$

This relationship has shown to be roughly linear for small saccades in the range of $0-10^\circ$ amplitude. As a result, we have assumed that a linear approximation is acceptable in the current context, as the saccades produced during reading are often on the order of $0-3^\circ$ amplitude, with very few over 10° amplitude.

To calculate the slope coefficient of this relationship, a data set was constructed from the saccade groups such that x-column data contained absolute component (horizontal or vertical) amplitude and y-column data contained the respective absolute component peak velocity.

The slope coefficient of the main sequence relationship was obtained from a linear regression of this data set.

3.3. Feature Comparison

Analysis of Scanpath Components. While the previously discussed metrics proved a means of quantifying certain features of individual scanpaths, additional calculations are necessary to compare the similarity of the metrics produced by different scanpaths.

To determine a relative measure of similarity between metrics, a Gaussian cumulative distribution function (CDF) was applied as follows, where x and μ are the metric values being compared and σ is the metric-specific standard deviation:

$$p = \frac{1}{\sigma\sqrt{2\pi}} \int_{-\infty}^x e^{-\frac{t-\mu}{2\sigma^2}} dt \quad (5)$$

Metric-specific standard deviations were determined empirically, details are given in the Experimental Setup section.

The Gaussian CDF comparison produces a probability value between 0 and 1, where a value of 0.5 indicates an exact match and a value of 0 or 1 indicates no match. This probability is converted into a more intuitive similarity score, where a value of 0 indicates no match and values of 1 indicates an exact match, with the following equation:

$$\text{Similarity} = 1 - |2p - 1| \quad (6)$$

From the similarity score, a simple acceptance threshold may be used to indicate the level of similarity which constitutes a biometric match.

Pairwise Distance Comparison. In addition to similarity calculations for the various scanpath metrics, a method of scanpath analysis similar to that described by Grindinger et al. [6] was developed to estimate the spatial similarity of two distinct scanpaths.

In comparing two scanpaths, the Euclidean pairwise distance was calculated between the centroid positions of fixations. Following this, a tally was made of the total number of fixation points in each set that could be matched to within 1° of at least one point in the opposing set. The similarity of scanpaths was assessed by the proportion of tallied fixation points to the total number of fixation points, to produce a similarity score similar to those generated for the various eye movement metrics.

3.4. Information Fusion

Information fusion combines the information obtained from different biometric traits to improve the overall accuracy of a biometric system [19].

The previously discussed similarity calculations produce a total of 15 different similarity scores based on varying aspects of scanpath analysis. To consolidate these results into a single representative biometric, we employed the use of a weighted mean formula, to improve the overall accuracy of identification while making allowance for the relative accuracy of individual features:

$$\text{Similarity} = \frac{\sum_{i=1}^n \text{Weight}_i \times \text{Similarity}_i}{\sum_{i=1}^n \text{Weight}_i} \quad (7)$$

Metric-specific weighting values were determined empirically, details are given in the Experimental Setup section.

4. Experimental Setup

4.1. Participants

Eye movement data was collected for a total of 32 subjects (26 males / 6 females), ages 18 – 40 with an average age of 23 (SD = 5.4). Mean positional accuracy of the recordings averaged between all calibration points was 0.74° (SD = 0.54°). 29 of the subjects performed 4 recordings each, and 3 of the subjects performed 2

recordings each, generating a total of 122 unique eye movement records.

The first two recordings for each subject were conducted during the same session with a 20 minute break between recordings; the second two recordings were performed a week later, again with a 20 minute break between recordings.

4.2. Apparatus & Software

Eye movements were recorded using an EyeLink II eye tracker [17] running at 1000 Hz. Stimuli were presented on a flat screen monitor positioned at a distance of roughly 685 millimeters from the subject, with screen dimensions of 640×400 millimeters, and resolution of 2560×1600 pixels.

All algorithms and data analysis were implemented and performed in MATLAB, and run using a 3.1 GHz quad-core CPU with 16 GB memory (DDR3 RAM).

4.3. Procedure

Eye movement records were generated for participants' readings of various excerpts from Lewis Carroll's "The Hunting of the Snark." This poem was chosen for its difficult and nonsensical content, forcing readers to progress slowly and carefully through the text.

For each recording, the participant was given 1 minute to read, and text excerpts were chosen to require roughly 1 minute to complete. To reduce learning effects, participants were given different excerpts for each recording session, each of which maintained similar line lengths throughout multiple reading sessions.

The raw eye movement records were then processed and classified into the fixations and saccades that describe their unique scanpaths. To determine the metric-specific standard deviation values to be used in similarity calculations, the various eye movement metrics were calculated for each recording, the standard deviation of each metric for recordings produced by each subject were calculated separately, and the average within-subject standard deviation (α) for each metric was calculated. Then, the standard deviation value used for metric-specific similarity calculations was twice the metric-specific average within-subject standard deviation:

$$\sigma = 2\alpha \quad (8)$$

To examine the relative accuracy of individual metrics as biometric features, similarity calculations were run for each metric across all possible combinations of eye movement records. For example, considering 3 eye movement records (A, B, and C) produced by unique subjects, similarity scores were produced for the combinations: A + B, A + C, B + C. For the 122 eye movement records, this resulted in:

$$\binom{122}{2} = 7381 \text{ combinations} \quad (9)$$

From these similarity scores, the receiver operating characteristic curves of individual metrics were plotted and equal error rates were determined to assess their relative accuracies and assign appropriate weighting values to the identification algorithm:

Weight	Similarity Metric
25	Fixation count
75	Average fixation duration
1	Average vectorial amplitude
10	Average horizontal amplitude
1	Average vertical amplitude
10	Average vectorial velocity
1	Average vectorial peak velocity
1	Velocity waveform indicator
1	Scanpath length
10	Scanpath area
1	Regions of interest
10	Inflection count
1	Amplitude-duration coefficient
1	Main sequence coefficient
1	Pairwise distance comparison

Table 1: Metric-specific weighting values.

The accuracy of the final identification algorithm was then calculated similar to metric-specific accuracy, followed by performance assessments of the various identification stages.

5. Results

5.1. Identification Accuracy

False acceptance rate (FAR) is defined as the percentage of erroneously matched similarity scores, and false rejection rate (FRR) is defined as the percentage of erroneously unmatched similarity scores. The receiver operating characteristic (ROC) curves, shown in Figure 4, plot false rejection rate against false acceptance rate at various acceptance thresholds. The equal error rate (EER), shown in Table 2, is the error rate at which false acceptance rate and false rejection rate are equal.

EER	Similarity Metric
34%	Fixation count
30%	Average fixation duration
42%	Average vectorial amplitude
36%	Average horizontal amplitude
46%	Average vertical amplitude

37%	Average vectorial velocity
43%	Average vectorial peak velocity
42%	Velocity waveform indicator
43%	Scanpath length
48%	Scanpath area
49%	Regions of interest
38%	Inflection count
45%	Amplitude-duration coefficient
49%	Main sequence coefficient
43%	Pairwise distance comparison
27%	Weighted mean

Table 2: Equal error rates.

Of the considered metrics, average fixation duration (30% EER), fixation count (34% EER), average horizontal saccade amplitude (36% EER), average vectorial saccade velocity (37% EER), and inflection count (38% EER) displayed the most accuracy as biometric indicators.

The main sequence coefficient (49% EER), regions of interest (49% EER), scanpath area (48% EER), and amplitude-duration coefficient (45% EER) provided the least accuracy, often reaching their best half total error rate (HTER) at an acceptance threshold of 1.0, indicating a very poor trade-off of FAR to FRR. It seems likely that this is due in part to the higher level of abstraction inherent in these metrics. While further refinement of thresholds and comparison techniques may yield better results, as presented these metrics do not provide adequate accuracy to justify their use as biometrics.

As well, the weighted mean fusion of scanpath features provides a clear and noticeable benefit in comparison to the individual metrics, as can be seen from the comparative ROC curves, achieving an EER of 27%.

5.2. Identification Performance

Averaged over 10 independent runs, the full process from eye movement classification to biometric identification for comparing the eye movement data supplied by two unique recordings (roughly 3 MB each) took less than 2.30 seconds (SD = 0.01). Of this, eye movement classification took 1.92 seconds (SD = 0.01), feature extraction took 0.35 seconds (SD = 0.01), feature comparison took 0.03 seconds (SD = 0.00), and information fusion took 0.00 seconds (SD = 0.00). Note that eye movement classification may be performed in real time as eye movement data is collected [9], removing this potential bottleneck from performance considerations.

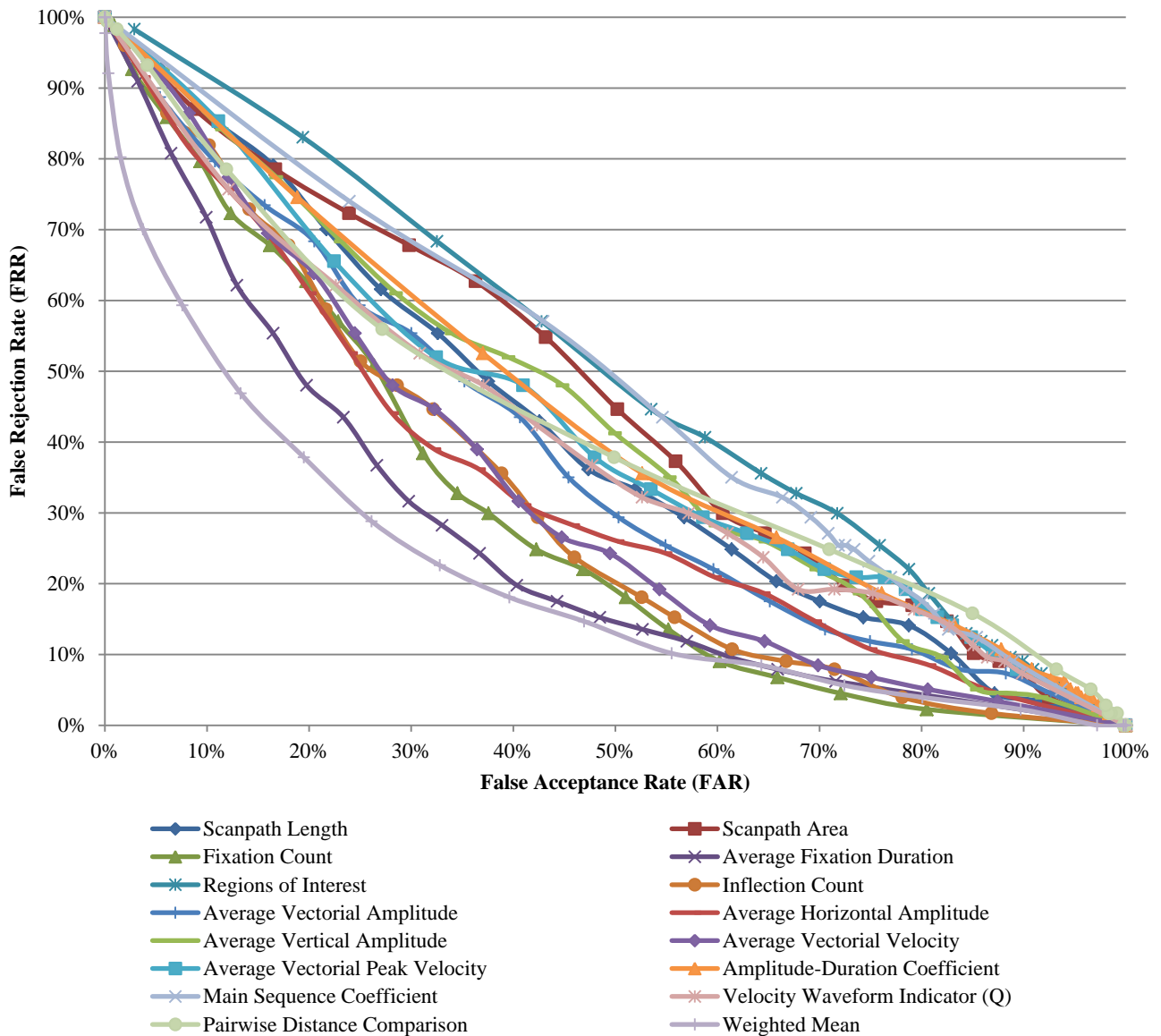


Figure 4: Receiver operating characteristics.

6. Limitations

The experiments presented in this paper were conducted under very controlled conditions with the use of high accuracy eye tracking equipment. In practice it would be difficult to replicate such ideal conditions. As well, the relatively small amount of tested subjects and data sets per subject increases the possibility of skewed accuracy results caused by random variation/similarity between recordings.

7. Future Research

There are a number of areas in which the accuracy of these metrics may be improved, including: adjustments to

the way analysis is performed, content related analysis, and the implications towards high level brain activity. While we have not addressed these issues in the current paper, focusing instead on the general applicability of scanpath metrics to biometric identification, they are worth noting as the possible subjects of continued research in this area.

7.1. Statistical Analysis Adjustments

Selection of more appropriate standard deviation values and comparison of different probability distributions (e.g. Gamma, Chi-square, etc.) for metric-specific similarity calculations may improve their respective error rates, while a thorough examination of the individual metrics and their relations may allow for increased accuracy through

information fusion as the metric-specific weighting values are optimized.

7.2. Content Related Analysis

In addition to the considered scanpath metrics, the eye movements produced during reading also exhibit certain traits that are not readily apparent in less structured patterns, allowing further metrics for scanpath comparison [21, 22]. These metrics include: the distribution of fixation positions within a word, which are often Gaussian with a center dependent on the word length; the relative amount of regressions (fixations on previously visited words); and the relative amount of skipped words (words not directly fixated on).

7.3. High Level Brain Activity

This work investigated the biometric potential of a set of basic measurements related to individual eye movements and aggregated scanpath characteristics. It is also important to understand if it is possible to categorize the motor control strategies employed by the brain for visual search and learning, and employ such information for identification purposes.

8. Conclusion

As technology advances, biometric traits are becoming easier to reproduce, circumventing the purposes of existing biometric identification techniques and leaving gaps in the efficacy of the systems that use them. Scanpath theory presents a unique solution, as eye movements are uniquely counterfeit resistant due to the complex neurological interactions and extraocular muscle properties involved in their generation.

This paper has presented an objective evaluation of a number of scanpath-based biometric features and their ability to accurately and precisely distinguish unique individuals, with equal error rates ranging from 30%–49%. As well, we have presented an information fusion method which allows for the combination of multiple metrics to produce more stable/accurate identification, which we have shown to be capable of producing an equal error rate of 27% with near real-time performance, allowing for the comparison of two pre-classified eye movement records in less than 0.5 seconds.

9. Acknowledgements

The work was partially funded by grant from the National Institute of Standards #60NANB10D213. Special gratitude is expressed to Dr. Alex Karpov for his assistance with data collection and processing.

10. References

- [1] Abdel-Mottaleb, M. and Zhou, J. Human Ear Recognition from Face Profile Images, 2005.
- [2] Bahill, A.T., Clark, M.R. and Stark, L. The main sequence, a tool for studying human eye movements. *Mathematical Biosciences*, 24(3-4): 191-204, 1975.
- [3] Cappelli, R., Maio, D., Maltoni, D., Wayman, J.L. and Jain, A.K. Performance Evaluation of Fingerprint Verification Systems. *IEEE Transactions on Pattern Analysis and Machine Intelligence*, 28(3-18), 2006.
- [4] Dorairaj, V., Schmid, N.A. and Fahmy, G. Performance evaluation of non-ideal iris based recognition system implementing global ICA encoding, 2005.
- [5] Goldberg, J.H. and Kotval, X.P. Computer interface evaluation using eye movements: methods and constructs. *International Journal of Industrial Ergonomics*, 24(6): 631-645, 1999.
- [6] Grindinger, T., Duchowski, A.T. and Sawyer, M. Group-wise similarity and classification of aggregate scanpaths, 2010.
- [7] Jain, A.K., Flynn, P. and Ross, A.A. *Handbook of Biometrics*, 2008.
- [8] Kasprowski, P. Human identification using eye movements, 2004.
- [9] Koh, D.H., Gowda, S.A.M. and Komogortsev, O.V. Input evaluation of an eye-gaze-guided interface: kalman filter vs. velocity threshold eye movement identification, 2009.
- [10] Komogortsev, O.V., Gobert, D.V., Jayarathna, S., Koh, D.H. and Gowda, S.M. Standardization of Automated Analyses of Oculomotor Fixation and Saccadic Behaviors. *IEEE Transactions on Biomedical Engineering*, 57(11): 2635-2645, 2010.
- [11] Komogortsev, O.V. and Khan, J.I. Eye movement prediction by Kalman filter with integrated linear horizontal oculomotor plant mechanical model, 2008.
- [12] Leigh, R.J. and Zee, D.S. *The Neurology of Eye Movements*, 2006.
- [13] Lu, J., Plataniotis, K.N. and Venetsanopoulos, A.N. Face Recognition Using LDA Based Algorithms. *IEEE Transactions on Neural Networks*, 14(1): 195-200, 2003.
- [14] Noton, D. and Stark, L. Scanpaths in Eye Movements during Pattern Perception. *Science*, 171(3968): 308-311, 1971.
- [15] Paulson, E.J. Viewing Eye Movements During Reading Through the Lens of Chaos Theory: How Reading Is Like the Weather. *Reading Research Quarterly*, 40(3): 338-358, 2005.
- [16] Rayner, K. Eye Movements in Reading and Information Processing: 20 Years of Research. *Psychological Bulletin*, 124(3): 372-422, 1998.
- [17] Research, S. EyeLink 1000. Supplied as additional material http://www.sr-research.com/EL_1000.html.
- [18] Roberts, C. Biometric attack vectors and defences. *Computers & Security*, 26(1): 14-25, 2007.
- [19] Ross, A. and Jain, A. Information fusion in biometrics. *Pattern Recognition Letters*, 24(13): 2115-2125, 2003.
- [20] Santella, A. and DeCarlo, D. Robust clustering of eye movement recordings for quantification of visual interest, 2004.
- [21] Schad, D.J., Nuthmann, A. and Engbert, R. Eye movements during reading of randomly shuffled text. *Vision Research*, 50(23): 2600-2616, 2010.

900	[22] Schnitzer, B.S. and Kowler, E. Eye movements during	950
901	multiple readings of the same text. Vision Research, 46(10):	951
902	1611-1632, 2006.	952
903	[23] Silver, D.L. and Biggs, A.J. Keystroke and Eye-Tracking	953
904	Biometrics for User Identification, 2008.	954
905		955
906		956
907		957
908		958
909		959
910		960
911		961
912		962
913		963
914		964
915		965
916		966
917		967
918		968
919		969
920		970
921		971
922		972
923		973
924		974
925		975
926		976
927		977
928		978
929		979
930		980
931		981
932		982
933		983
934		984
935		985
936		986
937		987
938		988
939		989
940		990
941		991
942		992
943		993
944		994
945		995
946		996
947		997
948		998
949		999